

DIFFRACTION OF SOUND FROM SEMI-INFINITE PERFORATED AND SEMI-INFINITE COATED DUCT WITH RING SOURCE

Burhan TIRYAKIOGLU

Department of Mathematics, Marmara University, Istanbul, TÜRKİYE

ABSTRACT. This study delves into the analysis of acoustic waves emanating from a ring source in an infinite cylindrical duct. The duct is equipped with an acoustically absorbing lining on its outer surface when z is less than l , and is perforated when z is greater than l . The inclusion of acoustically absorbing lining results in a substantial increase in the complexity of the equations compared to the scenario without such lining. Through rigorous efforts, these intricate equation systems are numerically solved, and graphs are generated across various parameter values. Furthermore, by adjusting the parameter values, a physical resemblance is established with an existing study in the literature, showcasing impeccable alignment in the results.

1. INTRODUCTION


In recent years, the problem of diffraction or radiation of sound waves has been a significant subject analyzed by researchers. Duct and pipe structures have a widespread application in industrial systems such as exhaust systems, ventilation systems, aircraft jets, and modern turbofan engines to control unwanted and potentially harmful noise. Therefore, there is a need to explore more precise mathematical models to address these complex engineering issues.

The Wiener–Hopf method [1], widely recognized for its convenience in analyzing such applications, is included in numerous studies within the literature [2–8]. First, Levine and Schwinger employed the Wiener–Hopf method to investigate the radiation of sound through a semi-infinite rigid duct [9].

There are some techniques used to reduce unwanted noise in duct and pipe modeling. Some of these methods include covering the entire or part of the duct

2020 *Mathematics Subject Classification.* 78A45, 47A68, 42B10.

Keywords. Absorbing lining, perforated duct, Wiener–Hopf, ring source.

✉ burhan.tiryakioglu@marmara.edu.tr;  0000-0003-1448-6147.

with acoustically absorbing lining [10–14] using expansion or contraction chambers [15, 16] and using perforated structures [17, 18].

This study is approached by taking inspiration from the previous study [19]. Unlike the previous one, an acoustically absorbing lining is utilized in this study. This change, although not creating a significant difference at first glance, can be said to transform the existing problem into a quite complex and practical one, especially with the use of acoustically absorbing lining. Significantly, this adjustment introduces a nuanced challenge, particularly evident in terms of mathematical analysis, where it yields a greater number of unknown functions and a binary system of equations. The primary objective of this research is to augment the existing perforated structure by introducing an acoustically absorbing lining. It is well-established that such linings contribute to a measurable reduction in sound pressure levels, typically by a few decibels. Consequently, the simultaneous utilization of both a perforated structure and an acoustically absorbing lining is posited as the key to achieving optimal efficiency in acoustic control.

This study consists of the following sections. In Section 2, the formulation of the problem and the presentation of boundary-continuity conditions are provided. Section 3 addresses the derivation and solution of the Wiener–Hopf equation. Far field analysis is performed in Section 4. In Section 5, numerical results are presented using graphics generated for various parameter values. Finally, Section 6 summarizes the findings obtained from solving the problem.

2. PROBLEM SETTING

The problem’s geometric configuration is illustrated in Figure 1. Here, the duct walls are modeled as infinitely thin, occupying the region $\{r = a, z \in (-\infty, \infty)\}$, illuminated by a ring source [20] situated at $\{r = b, z = -c, c > 0\}$. For $z < l$, the exterior surface of the cylinder assumes an acoustically absorbing lining characterized by Z , while the interior surface is assumed to be rigid. The duct for $z > l$ is considered perforated. Due to the symmetry of both the problem’s geometry and the ring source, the total field remains independent of azimuth ϕ throughout the circular cylindrical coordinate system (r, ϕ, z) .

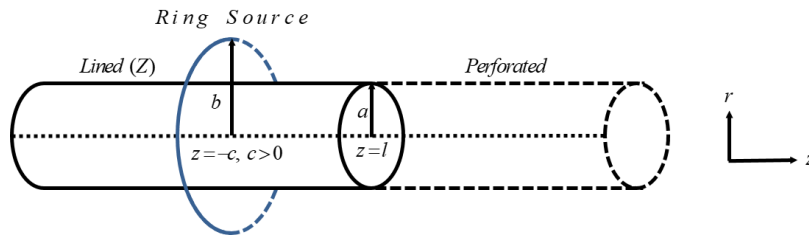


FIGURE 1. The geometry of the problem.

The scalar potential $\psi(r, z)$ can be ascertained by establishing a relationship between velocity v and acoustic pressure p , as expressed by the following equations. $\vec{v} = \text{grad } \psi$ and $p = \rho_0 \partial \psi / \partial t$, where ρ_0 represents the density of the undisturbed medium, and t denotes time. In the course of this study, we assume a harmonic time dependence of the form $e^{-i\omega t}$, where ω stands for the angular frequency.

For analytical simplicity, the total field $\psi_t(r, z)$ can be represented as:

$$\psi_t(r, z) = \begin{cases} \psi_1(r, z), & r > b \\ \psi_2(r, z), & a < r < b \\ \psi_3(r, z), & r < a \end{cases}, \quad (1)$$

where $\psi_j(r, z)$, $j = 1, 2, 3$ appearing in (1) are an unknown functions that satisfy the wave equation

$$\left[\frac{1}{r} \frac{\partial}{\partial r} \left(r \frac{\partial}{\partial r} \right) + \frac{\partial^2}{\partial z^2} + k^2 \right] \psi_j(r, z) = 0, \quad j = 1, 2, 3. \quad (2)$$

Here, $k = \omega/c_0$ represents the wavenumber, where ω is the angular frequency, and c_0 is the speed of sound.

From the geometry of the problem, one can write the following boundary conditions and continuity relations. The outer surface of the duct is lined with acoustically absorbing lining for $z < l$, this means

$$\left(\frac{ik}{Z} - \frac{\partial}{\partial r} \right) \psi_2(a, z) = 0, \quad z < l, \quad (3)$$

where Z denotes the acoustic impedance of the lined wall. The inner surface of the duct is rigid for $z < l$, one obtains

$$\frac{\partial}{\partial r} \psi_3(a, z) = 0, \quad z < l. \quad (4)$$

For the perforated duct for $z > l$, the following conditions can be written

$$\begin{aligned} \frac{\partial}{\partial r} \psi_2(a, z) &= \frac{\partial}{\partial r} \psi_3(a, z), \quad z > l \\ \psi_2(a, z) &= \psi_3(a, z) + i \frac{\zeta_p}{k} \frac{\partial}{\partial r} \psi_3(a, z), \quad z > l \end{aligned}, \quad (5)$$

where ζ_p is the specific impedance [21], which characterizes the acoustic properties of the perforated duct.

$$\zeta_p = [0.006 - ik(t_w + 0.75d_h)]/\sigma,$$

with t_w representing the screen thickness, d_h denoting the perforate hole diameter, and σ indicating the porosity.

The last following conditions can be obtained from the ring source

$$\begin{aligned} \frac{\partial}{\partial r} \psi_1(b, z) - \frac{\partial}{\partial r} \psi_2(b, z) &= \delta(z + c), \quad z \in (-\infty, \infty), \\ \psi_1(b, z) - \psi_2(b, z) &= 0, \quad z \in (-\infty, \infty) \end{aligned} \quad (6)$$

where δ represents the Dirac delta function.

By taking Fourier transform of (2) we obtain the following integral representations

$$\begin{aligned} \psi_1(r, z) &= \frac{k}{2\pi} \int_{\mathcal{L}} A(\alpha) H_0^{(1)}(\lambda kr) e^{-i\alpha kz} d\alpha \\ \psi_2(r, z) &= \frac{k}{2\pi} \int_{\mathcal{L}} [B(\alpha) J_0(\lambda kr) + C(\alpha) Y_0(\lambda kr)] e^{-i\alpha kz} d\alpha, \\ \psi_3(r, z) &= \frac{k}{2\pi} \int_{\mathcal{L}} D(\alpha) J_0(\lambda kr) e^{-i\alpha kz} d\alpha \end{aligned} \quad (7)$$

In the context where $A(\alpha)$, $B(\alpha)$, $C(\alpha)$, and $D(\alpha)$ are the spectral coefficients, determined by solving the equations (3)-(6), the integration contour \mathcal{L} is chosen to be a suitable inverse Fourier transform along or near the real axis in the complex α -plane. The functions J_0 and Y_0 correspond to the Bessel and Neumann functions of order zero, respectively. Additionally, $H_0^{(1)} = J_0 + iY_0$ represents the Hankel function of the first type [22], while λ stands for the square root function, defined as:

$$\lambda(\alpha) = \sqrt{1 - \alpha^2}, \quad \lambda(0) = 1.$$

3. WIENER-HOPF PROCEDURE

In this section, the Wiener-Hopf equation will be derived and the solution obtained.

3.1. Derivation of the Wiener-Hopf Equations. Enforcing the boundary conditions at $r = a$ and performing Fourier transforms of (3) and (4) yields:

$$k[B(\alpha)J(Z, \alpha) + C(\alpha)Y(Z, \alpha)] = e^{i\alpha kl} \Phi_1^+(\alpha), \quad (8)$$

$$-\lambda k D(\alpha) J_1(\lambda ka) = e^{i\alpha kl} \Phi_2^+(\alpha), \quad (9)$$

where

$$J(Z, \alpha) = iJ_0(\lambda ka)/Z + \lambda J_1(\lambda ka),$$

$$Y(Z, \alpha) = iY_0(\lambda ka)/Z + \lambda Y_1(\lambda ka).$$

Similarly, from equation (5), we get

$$-\lambda k D(\alpha) J_1(\lambda ka) + \lambda k B(\alpha) J_1(\lambda ka) + \lambda k C(\alpha) Y_1(\lambda ka) = e^{i\alpha kl} \Phi_1^-(\alpha), \quad (10)$$

$$D(\alpha) [J_0(\lambda ka) - i\lambda \zeta_p J_1(\lambda ka)] - B(\alpha) J_0(\lambda ka) - C(\alpha) Y_0(\lambda ka) = e^{i\alpha kl} \Phi_2^-(\alpha). \quad (11)$$

In the upper half-plane, $\Phi_{1,2}^+$, and in the lower half-plane, $\Phi_{1,2}^-$ are analytical functions, as described in [19], and their definitions are as follows:

$$\begin{aligned}\Phi_1^+(\alpha) &= \int_l^\infty \left[\frac{ik}{Z} \psi_2(a, z) - \frac{\partial}{\partial r} \psi_2(a, z) \right] e^{i\alpha k(z-l)} dz \\ \Phi_2^+(\alpha) &= \int_l^\infty \frac{\partial}{\partial r} \psi_3(a, z) e^{i\alpha k(z-l)} dz \\ \Phi_1^-(\alpha) &= \int_{-\infty}^l \left[\frac{\partial}{\partial r} \psi_3(a, z) - \frac{\partial}{\partial r} \psi_2(a, z) \right] e^{i\alpha k(z-l)} dz \\ \Phi_2^-(\alpha) &= \int_{-\infty}^l [\psi_3(a, z) - \psi_2(a, z)] e^{i\alpha k(z-l)} dz\end{aligned}$$

Finally, from the ring source on $r = b$, we obtain

$$\lambda k A(\alpha) H_1^{(1)}(\lambda kb) = \lambda k B(\alpha) J_1(\lambda kb) + \lambda k C(\alpha) Y_1(\lambda kb) - e^{-i\alpha kc}, \quad (12)$$

$$A(\alpha) H_0^1(\lambda kb) = B(\alpha) J_0(\lambda kb) + C(\alpha) Y_0(\lambda kb), \quad (13)$$

where $H_0^{(1)} = J_1 + Y_1$. By using the above two equation (12) and (13), one gets

$$\begin{aligned}B(\alpha) &= A(\alpha) + e^{-i\alpha kc} \frac{\pi b}{2} Y_0(\lambda kb) \\ C(\alpha) &= iA(\alpha) - e^{-i\alpha kc} \frac{\pi b}{2} J_0(\lambda kb).\end{aligned} \quad (14)$$

The coefficients $A(\alpha)$, $B(\alpha)$, and $C(\alpha)$ are interrelated through the equation (14), whereas the coefficient $D(\alpha)$ can be readily derived from the equation (9).

$$D(\alpha) = -\frac{e^{i\alpha kl} \Phi_2^+(\alpha)}{\lambda k J_1(\lambda ka)}. \quad (15)$$

By using (8) and (14), $A(\alpha)$ can be obtained as follows

$$A(\alpha) = \frac{e^{i\alpha kl} \Phi_1^+(\alpha)}{kH(Z, \alpha)} - \frac{e^{-i\alpha kc} \pi b}{2H(Z, \alpha)} [Y_0(\lambda kb) J(Z, \alpha) - J_0(\lambda kb) Y(Z, \alpha)], \quad (16)$$

where

$$H(Z, \alpha) = iH_0^{(1)}(\lambda ka)/Z + \lambda H_1^{(1)}(\lambda ka).$$

By substituting these coefficients ($A(\alpha)$, $B(\alpha)$, $C(\alpha)$ and $D(\alpha)$) into (5), we obtain the following equations

$$\Phi_2^+(\alpha) + \frac{\lambda H_1^{(1)}(\lambda ka)}{H(Z, \alpha)} \Phi_1^+(\alpha) + \frac{ib}{aZ} e^{-i\alpha k(c+l)} \frac{H_0^{(1)}(\lambda kb)}{H(Z, \alpha)} = \Phi_1^-(\alpha), \quad (17)$$

$$\begin{aligned}-\frac{J_0(\lambda ka) - i\lambda \zeta_p J_1(\lambda ka)}{\lambda k J_1(\lambda ka)} \Phi_2^+(\alpha) - \frac{H_0^{(1)}(\lambda ka)}{kH(Z, \alpha)} \Phi_1^+(\alpha) + \frac{b}{ka} e^{-i\alpha k(c+l)} \frac{H_0^{(1)}(\lambda kb)}{H(Z, \alpha)} \\ = \Phi_2^-(\alpha).\end{aligned} \quad (18)$$

$H_0^{(1)}(\lambda ka)/H(Z, \alpha)$ can be eliminated from equations (17) and (18), we get

$$\Phi_1^+(\alpha) + L(\alpha)\Phi_2^+(\alpha) = \left[\Phi_1^-(\alpha) - \frac{ik}{Z}\Phi_2^-(\alpha) \right], \quad (19)$$

where

$$L(\alpha) = \frac{J(Z, \zeta_p, \alpha)}{\lambda J_1(\lambda ka)}, \quad (20)$$

and

$$J(Z, \zeta_p, \alpha) = J(Z, \alpha) + \zeta_p J_1(\lambda ka)/Z.$$

Then eliminating $\Phi_2^+(\alpha)$ from equation (18) and (19), we get

$$\begin{aligned} \Phi_1^+(\alpha)M(\alpha) + \frac{b}{a} \frac{H_0^{(1)}(\lambda kb)}{H(Z, \alpha)} e^{-i\alpha k(c+l)} \\ = \left[\Phi_1^-(\alpha) - \frac{ik}{Z}\Phi_2^-(\alpha) \right] \frac{J_0(\lambda ka) - i\lambda\zeta_p J_1(\lambda ka)}{J(Z, \zeta_p, \alpha)} + k\Phi_2^-(\alpha), \end{aligned} \quad (21)$$

where

$$M(\alpha) = \frac{J_0(\lambda ka) - i\lambda\zeta_p J_1(\lambda ka)}{J(Z, \zeta_p, \alpha)} - \frac{H_0^{(1)}(\lambda ka)}{H(Z, \alpha)}. \quad (22)$$

(19) and (21) are two coupled Wiener–Hopf equations and $L(\alpha)$, $M(\alpha)$ are kernel functions given in (20) and (22), respectively, to be factorized.

3.2. Solution of the Wiener–Hopf Equations. Examine the first Wiener–Hopf equation in (19) and reorganize it using (20) in the subsequent format:

$$\frac{\lambda J_1(\lambda ka)}{J(Z, \zeta_p, \alpha)} \Phi_1^+(\alpha)L_+(\alpha) + \Phi_2^+(\alpha)L_+(\alpha) = \left[\Phi_1^-(\alpha) - \frac{ik}{Z}\Phi_2^-(\alpha) \right] L_-(\alpha). \quad (23)$$

Similarly, by using equation (21) and (22), we get

$$\begin{aligned} \Phi_1^+(\alpha)M_+(\alpha) + \frac{b}{a} \frac{H_0^{(1)}(\lambda kb)}{H(Z, \alpha)} e^{-i\alpha k(c+l)} M_-(\alpha) \\ = \left[\Phi_1^-(\alpha) - \frac{ik}{Z}\Phi_2^-(\alpha) \right] \frac{J_0(\lambda ka) - i\lambda\zeta_p J_1(\lambda ka)}{J(Z, \zeta_p, \alpha)} M_-(\alpha) + k\Phi_2^-(\alpha)M_-(\alpha). \end{aligned} \quad (24)$$

Here, $L_+(\alpha)$, $M_+(\alpha)$, $L_-(\alpha)$, and $M_-(\alpha)$ represent analytic functions devoid of zeros in the upper and lower half-planes, respectively. The factorization of $L(\alpha)$ and $M(\alpha)$ is provided as follows [19]:

$$L(\alpha) = \frac{L_+(\alpha)}{L_-(\alpha)}, \quad M(\alpha) = \frac{M_+(\alpha)}{M_-(\alpha)}.$$

In the upper half-plane, the left-hand side of (23) is analytic, except for the poles originating from the zeros of $J(Z, \zeta_p, \alpha)$ situated in the same half-plane, specifically at $\alpha = \alpha_m^-$ with

$$iJ_0 \left(\sqrt{1 - (\alpha_m^-)^2} ka \right) / Z + \sqrt{1 - (\alpha_m^-)^2 + \zeta_p} / Z J_1 \left(\sqrt{1 - (\alpha_m^-)^2} ka \right) = 0. \quad (25)$$

By subtracting the infinite system of poles from both sides of (23), we obtain:

$$\begin{aligned} \frac{\lambda J_1(\lambda ka)}{J(Z, \zeta_p, \alpha)} \Phi_1^+(\alpha) L_+(\alpha) - \sum_{m=1}^{\infty} \frac{c_m^+}{\alpha - \alpha_m^-} + \Phi_2^+(\alpha) L_+(\alpha) \\ = \left[\Phi_1^-(\alpha) - \frac{ik}{Z} \Phi_2^-(\alpha) \right] L_-(\alpha) - \sum_{m=1}^{\infty} \frac{c_m^+}{\alpha - \alpha_m^-}, \end{aligned} \quad (26)$$

where

$$c_m^+ = \Phi_1^+(\alpha_m^-) L_+(\alpha_m^-) \lim_{\alpha \rightarrow \alpha_m^-} \frac{\lambda J_1(\lambda ka)}{\frac{d}{d\alpha} J(Z, \zeta_p, \alpha)}. \quad (27)$$

By applying the analytical continuation principle along with Liouville's theorem to (26), one obtains:

$$\left[\Phi_1^-(\alpha) - \frac{ik}{Z} \Phi_2^-(\alpha) \right] = \frac{1}{L_-(\alpha)} \sum_{m=1}^{\infty} \frac{c_m^+}{\alpha - \alpha_m^-}. \quad (28)$$

By applying similar procedure to (24), we get the followings

$$\Phi_1^+(\alpha) M_+(\alpha) = I_+(\alpha) + \sum_{m=1}^{\infty} \frac{c_m^-}{\alpha - \alpha_m^+}, \quad (29)$$

where

$$I(u) = -\frac{b}{a} \frac{H_0^{(1)}(\lambda kb)}{H(Z, \alpha)} e^{-i\alpha k(c+l)} M_-(\alpha) = I_+(\alpha) + I_-(\alpha), \quad (30)$$

and

$$c_m^- = \left[\Phi_1^-(\alpha_m^+) - \frac{ik}{Z} \Phi_2^-(\alpha_m^+) \right] M_-(\alpha_m^+) \lim_{\alpha \rightarrow \alpha_m^+} \frac{J_0(\lambda ka) - i\lambda \zeta_p J_1(\lambda ka)}{\frac{d}{d\alpha} J(Z, \zeta_p, \alpha)}. \quad (31)$$

Through the decomposition of (30), we can derive analytical functions in both the upper and lower half planes, given by $I(\alpha) = I_+(\alpha) + I_-(\alpha)$.

$$I_+(u) = -\frac{1}{2\pi i} \frac{b}{a} \int_{\mathcal{L}^+} \frac{H_0^{(1)}(\lambda kb) M_-(\tau)}{H(Z, \tau)(\tau - \alpha)} e^{-i\tau k(c+l)} d\tau. \quad (32)$$

3.3. Determining the Coefficient c_m^+ and c_m^- . Wiener–Hopf solutions (28) and (29) involve unknown coefficients c_m^+ and c_m^- that need to be determined. By substituting $\alpha = \alpha_n^+$ into (28) and utilizing the relation in (31), we get:

$$\frac{1}{M_-(\alpha_n^+) \lim_{\alpha \rightarrow \alpha_n^+} \frac{J_0(\lambda ka) - i\lambda \zeta_p J_1(\lambda ka)}{\frac{d}{d\alpha} J(Z, \zeta_p, \alpha)}} c_n^- = \frac{1}{L_-(\alpha_n^+)} \sum_{m=1}^{\infty} \frac{c_m^+}{\alpha_n^+ - \alpha_m^-}, \quad n = 1, 2, \dots \quad (33)$$

Similarly, by substituting $\alpha = \alpha_n^-$ into (29) and utilizing the relation in (27), we obtain:

$$\frac{M_+(\alpha_n^-)}{L_+(\alpha_n^-) \lim_{\alpha \rightarrow \alpha_n^-} \frac{\lambda J_1(\lambda ka)}{\frac{d}{d\alpha} J(Z, \zeta_p, \alpha)}} c_n^+ = I_+(\alpha_n^-) + \sum_{m=1}^{\infty} \frac{c_m^-}{\alpha_n^- - \alpha_m^+}, \quad n = 1, 2, \dots \quad (34)$$

To find the unknown coefficients c_m^+ and c_m^- , numerical solutions will be obtained for these coupled systems of algebraic equations. Given the rapid convergence of the infinite series, truncation can be efficiently performed. Therefore, all numerical results will be obtained by truncating the infinite series and the infinite systems of linear algebraic equations after the first N terms. As shown in Figure 2, it was observed that the amplitude of the diffracted field becomes insensitive to the increase in the truncation number after reaching $N = 15$ [23, 24].

4. FAR FIELD

The expression for the total field in the region $r > b$ can be derived from (7).

$$\psi_1(r, z) = \frac{k}{2\pi} \int_{\mathcal{L}} A(\alpha) H_0^{(1)}(\lambda kr) e^{-i\alpha kz} d\alpha. \quad (35)$$

By using (16) and (29), the total field can be formulated in the following manner:

$$\psi_1(r, z) = \psi_d(r, z) + \psi_i(r, z) + \psi_r(r, z), \quad (36)$$

where

$$\psi_d(r, z) = \frac{k}{2\pi} \int_{\mathcal{L}} \frac{\Phi_1^+(\alpha)}{kH(Z, \alpha)} H_0^{(1)}(\lambda kr) e^{-i\alpha kz} d\alpha, \quad (37)$$

$$\begin{aligned} & \psi_i(r, z) + \psi_r(r, z) \\ &= -\frac{kb}{4i} \int_{\mathcal{L}} \frac{Y_0(\lambda kb) J(Z, \alpha) - J_0(\lambda kb) Y(Z, \alpha)}{H(Z, \alpha)} H_0^{(1)}(\lambda kr) e^{-i\alpha k(z+c)} d\alpha. \end{aligned} \quad (38)$$

Substituting the following asymptotic expressions, valid for $kr \gg 1$, for $H_0^{(1)}(\lambda kr)$ and $J_0(\lambda kb)$ in place of them

$$H_0^{(1)}(\lambda kr) \sim \sqrt{\frac{2}{\pi \lambda kr}} e^{i(\lambda kr - \pi/4)},$$

and employing the saddle point technique [25], we obtain:

$$\psi_1(r, z) = \psi_d(R_1, \theta_1) + \psi_i(R_2, \theta_2) + \psi_r(R_2, \theta_2), \quad (39)$$

where

$$\psi_d(R_1, \theta_1) = -\frac{i}{\pi} \frac{\Phi_1^+(-\cos \theta_1)}{H(Z, -\cos \theta_1)} \frac{e^{ikR_1}}{kR_1}, \quad (40)$$

$$\begin{aligned} & \psi_i(R_2, \theta_2) + \psi_r(R_2, \theta_2) \\ &= \frac{ikb Y_0(kb \sin \theta_2) J(Z, -\cos \theta_2) - J_0(kb \sin \theta_2) Y(Z, -\cos \theta_2)}{2 H(Z, -\cos \theta_2)} \frac{e^{ikR_2}}{kR_2}. \end{aligned} \quad (41)$$

Φ_1^+ is given in (29). Here, R_1, θ_1 and R_2, θ_2 represent the spherical coordinates defined as follows:

$$\begin{aligned} r &= R_1 \sin \theta_1, & z - l &= R_1 \cos \theta_1, \\ r &= R_2 \sin \theta_2, & z + c &= R_2 \cos \theta_2. \end{aligned}$$

5. NUMERICAL RESULTS

In this section, graphs are produced for different parameter values by taking advantage of the properties of geometry. Some parameter values are taken as unchanged and given in Table 1. The values taken for different parameter values are selected from some studies in the literature [19,21]. Figures are produced using the Sound Pressure Level (SPL) formula defined below.

$$\text{SPL} = 20 \log_{10} \left| \frac{p}{2 \cdot 10^{-5}} \right|.$$

TABLE 1. The values of the parameter.

Truncation number	N	15
Density of Un. Med.	ρ_0	1.255 kg/m ³
Speed of sound	c_0	340 m/s
Screen thickness	t_w	0.00081 m
Hole diameter	d_h	0.0249 m
Ring source axis	c	0.050 m
Lining length	l	0.010 m
Far radius	R	46 m

In Figure 2, the sound pressure level is plotted according to the increase in truncation number (N) values. As can be seen, after a certain value of N , the change in sound pressure level is insignificant. Therefore, other graphs are produced for $N = 15$.

The change of sound pressure level according to both duct radius and ring source radius are plotted in Figure 3 and Figure 4, respectively. As expected, the sound

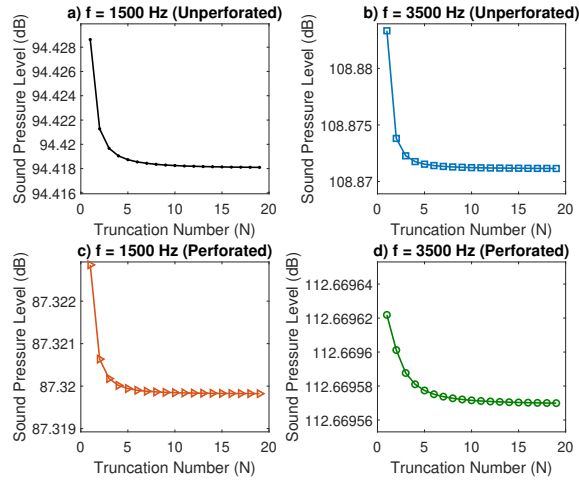


FIGURE 2. Sound Pressure Level (SPL) against the truncation number (N) for $a = 0.010$ m, $b = 0.075$ m, $Z = 1 - 2i$ and $\sigma = 0.057$.

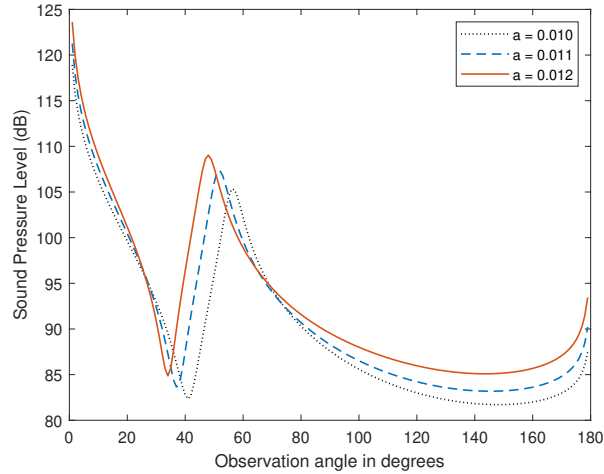


FIGURE 3. The impact of varied duct radius values (a) on Sound Pressure Level (SPL) at different observation angles, with fixed parameters: $f = 1500$ Hz, $b = 0.075$ m, $Z = 1 - 2i$, and $\sigma = 0.057$.

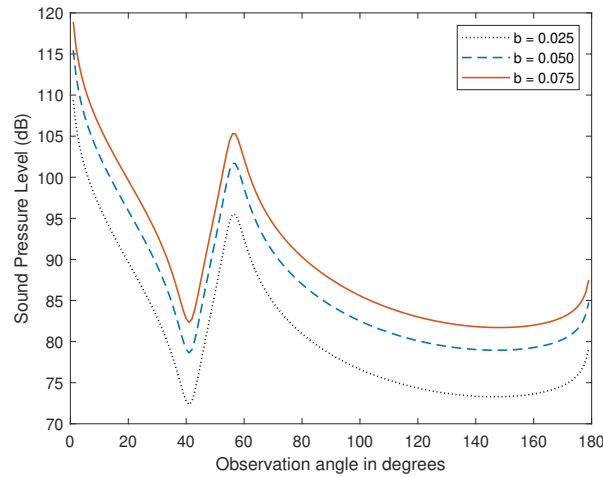


FIGURE 4. The impact of varied ring source radius values (b) on Sound Pressure Level (SPL) at different observation angles, with fixed parameters: $f = 1500$ Hz, $a = 0.010$ m, $Z = 1 - 2i$, and $\sigma = 0.057$.

pressure level increases with increasing the values of duct radius and ring source radius. On the other hand, the opposite situation exists for increasing values of c and l . As in the previous study [19], a decrease in the sound pressure level is observed both as the ring source moves away and as the duct extension increases.

The effect of acoustically absorbing lining is examined in Figure 5 and Figure 6. In Figure 5, the real part is kept constant for the complex impedance value, and the variation of sound pressure level is plotted with respect to the imaginary part. In Figure 6, the imaginary part is kept constant, and the variation of sound pressure level is plotted with respect to the real part. As seen, a decrease in sound pressure level can be achieved by selecting appropriate $\Re Z$ and $\Im Z$ values.

Figure 7 depicts the variation in sound pressure level for different porosity rates. As expected, the sound pressure level increases with an increase in porosity.

Consistency with the previous study [19] is examined in the last two graphs. These comparison figures indicate a meticulous handling of complex problems that particularly emerged in this study. In Figure 8, the impact of the lining is eliminated to establish physical similarity with the previous study. For this purpose, the impedance value is taken to infinity to obtain a graph for the rigid surface. It should be noted that the sound pressure level graphs obtained by taking the impedance value to infinity are identical to the previous ones. A similar situation holds true for Figure 9 as well. In this graph, normalized values of ka , kb , kc , and kl are employed for consistency with the previous study. To achieve physical similarity,

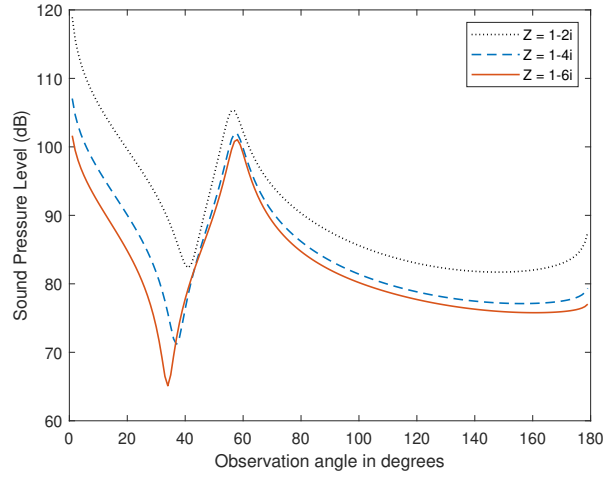


FIGURE 5. The impact of varied absorbing lining (reactance) values ($\Im m Z$) on Sound Pressure Level (SPL) at different observation angles, with fixed parameters: $f = 1500$ Hz, $a = 0.010$ m, $b = 0.075$ m, and $\sigma = 0.057$.

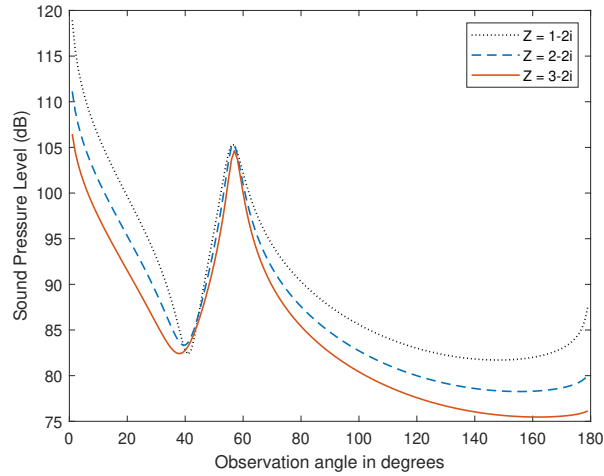


FIGURE 6. The impact of varied absorbing lining (resistance) values ($\Re e Z$) on Sound Pressure Level (SPL) at different observation angles, with fixed parameters: $f = 1500$ Hz, $a = 0.010$ m, $b = 0.075$ m, and $\sigma = 0.057$.

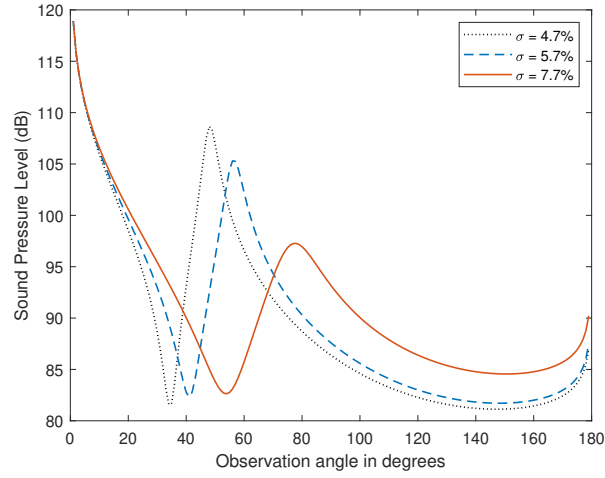


FIGURE 7. The impact of varied porosity values (σ) on Sound Pressure Level (SPL) at different observation angles, with fixed parameters: $f = 1500$ Hz, $a = 0.010$ m, $b = 0.075$ m and $Z = 1 - 2i$.

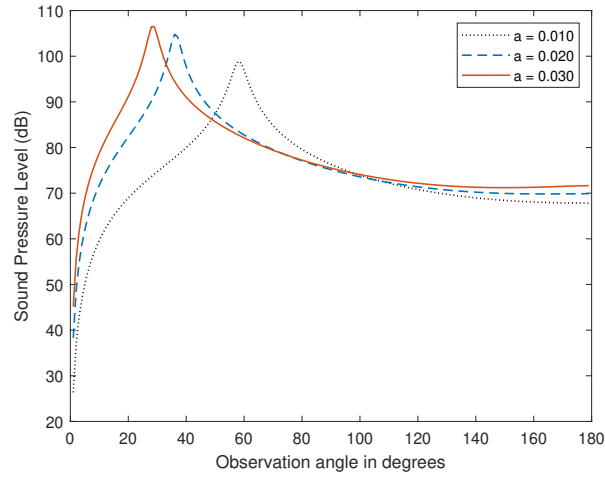


FIGURE 8. At parameters $f = 1500$ Hz, $a = 0.010$ m, $b = 0.075$ m, $Z \rightarrow \infty$, and $\sigma = 0.057$, comparison of the Sound Pressure Level (SPL) with different duct radius values (a) with the study of [19].

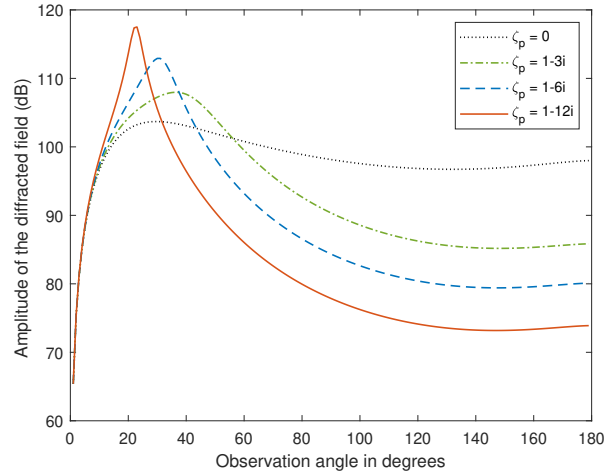


FIGURE 9. At parameters $ka = 1$, $kb = 10$, $kc = 6$, $kl = 10$ and $Z \rightarrow \infty$, comparison of the Sound Pressure Level (SPL) with open perforated duct with the study of [19].

the impedance value is taken to infinity. The obtained result, as in the previous graph, demonstrates very good alignment.

6. CONCLUSIONS

In this study, the diffraction of sound waves emanating from a ring source in an infinite duct with an acoustically lined outer surface for $z < l$ and a perforated surface for $z > l$ has been investigated using the Wiener Hopf technique. Due to the symmetry of both the problem's geometry and the ring source, the problem has been modeled in two dimensions. By solving the Wiener-Hopf equation, a solution is obtained. Graphs are presented for some specific values of problem parameters, such as the radius of the duct and the ring source, the effect of acoustically absorbing lining, and the perforated duct, to better understand their impact on the sound pressure level. An increase in the values of the duct radius (a) and the ring source radius (b) is observed to result in an increase in the sound pressure level. A similar trend is valid for both real and complex values of acoustically absorbing lining (Z). The effect of the perforated duct on the sound pressure level is also significant, with a decrease in the sound pressure level observed as the porosity of the perforated duct decreases. Finally, when compared to the study of [19] for $Z \rightarrow \infty$, it is observed that the conformity is excellent.

This study can also be used to consider the case where mean flow is present both inside and outside the duct. It is worth noting that when mean flow is included,

the current problem will be much more complicated to solve analytically and will require careful analysis.

Declaration of Competing Interests The author has no competing interests to declare.

REFERENCES

- [1] Noble, B., *Methods Based on the Wiener-Hopf Techniques*, Pergamon Press, London, 1958.
- [2] Rawlins, A.D., Wave propagation in a bifurcated impedance-lined cylindrical waveguide, *Journal of Engineering Mathematics*, 59 (2007), 419–435. <https://doi.org/10.1007/s10665-007-9172-4>
- [3] Rienstra, S.W., Acoustic scattering at a hard-soft lining transition in a flow duct, *Journal of Engineering Mathematics*, 59 (2007), 451–475. <https://doi.org/10.1007/s10665-007-9193-z>
- [4] Peake, N., Abrahams, I.D., Sound radiation from a semi-infinite lined duct, *Wave Motion*, 92 (2020), 102407. <https://doi.org/10.1016/j.wavemoti.2019.102407>
- [5] Hussain, S., Ayub, M., & Nawaz, R., Analysis of high frequency EM-waves diffracted by a finite strip with impedance in anisotropic medium, *Waves in Random and Complex Media*, (2021), 1–19. <https://doi.org/10.1080/17455030.2021.2000670>
- [6] Tiryakioglu, A., Tiryakioglu, B., Acoustic wave radiation from a coaxial pipe with partial lining and inner perforated screen, *International Journal of Aeroacoustics*, 22 (2023), 278–292. <https://doi.org/10.1177/1475472X231183152>
- [7] Alkinidri, M., Hussain, S., & Nawaz, R., Analysis of Noise Attenuation through Soft Vibrating Barriers: An Analytical Investigation, *AIMS Mathematics*, 8 (2023), 18066–18087. <https://doi.org/10.3934/math.2023918>
- [8] Hussain, S., Javaid, A., Alahmadi, H., Nawaz, R., & Alkinidri, M., A mathematical study of electromagnetic waves diffraction by a slit in non-thermal plasma, *Optical and Quantum Electronics*, 56 (2024), 213. <https://doi.org/10.1007/s11082-023-05730-8>
- [9] Levine, H., Schwinger, J., On the radiation of sound from an unflanged circular pipe, *Physical Review*, 73 (1948), 383–406. <https://doi.org/10.1103/PhysRev.73.383>
- [10] Rawlins, A.D., Radiation of sound from an unflanged rigid cylindrical duct with an acoustically absorbing internal surface, *Proc. Roy. Soc. Lond. A.*, 361 (1978), 65–91. <https://doi.org/10.1098/rspa.1978.0092>
- [11] Demir, A., Rienstra, S., Sound Radiation from a Lined Exhaust Duct with Lined Afterbody, *16th AIAA/CEAS Aeroacoustics Conference*, (2010) pp. 1–18, Stockholm, Sweden.
- [12] Demir, A., Buyukaksoy, A., Radiation of plane sound waves by a rigid circular cylindrical pipe with a partial internal impedance loading, *Acta Acustica United with Acustica*, 89 (2003), 578–585.
- [13] Safdar, M., Ahmed, N., Afzal, M., & Wahab, A., Acoustic scattering in lined panel cavities with membrane interfaces, *The Journal of the Acoustical Society of America*, 154 (2023), 1138–1151. <https://doi.org/10.1121/10.0020724>
- [14] Tiryakioglu, B., Analysis of sound transmission loss in an infinite duct with three different finite linings, *International Journal of Modern Physics B*, (2023), 2450384. <https://doi.org/10.1142/S0217979224503843>
- [15] Demir, A., Büyüaksoy, A., Transmission of sound waves in a cylindrical duct with an acoustically lined muffler, *International Journal of Engineering Science*, 41 (2003), 2411–2427. [https://doi.org/10.1016/S0020-7225\(03\)00240-4](https://doi.org/10.1016/S0020-7225(03)00240-4)
- [16] Demir, A., Büyüaksoy, A., Wiener–Hopf approach for predicting the transmission loss of a circular silencer with a locally reacting lining, *International Journal of Engineering Science*, 43 (2005), 398–416. <https://doi.org/10.1016/j.ijengsci.2004.12.003>

- [17] Nilsson, B., Brander, O., The propagation of sound in cylindrical ducts with mean flow and bulk-reacting lining I. modes in an infinite duct, *IMA Journal of Applied Mathematics*, 26 (1980), 269–298. <https://doi.org/10.1093/imamat/26.3.269>
- [18] Tiryakioglu, B., Radiation of acoustic waves by a partially lined pipe with an interior perforated screen. *Journal of Engineering Mathematics*, 122 (2020), 17–29. <https://doi.org/10.1007/s10665-020-10042-x>
- [19] Tiryakioglu, B., The effect of semi perforated duct on ring sourced acoustic diffraction, *Communications Faculty of Sciences University of Ankara Series A1 Mathematics and Statistics*, 70 (2021), 1073–1084. <https://doi.org/10.31801/cfsuasmas.699831>
- [20] Jones, D. S., *Acoustic and Electromagnetic Waves*, Clarendon Press , Oxford, 1986.
- [21] Sullivan, J.W., Crocker, M.J., Analysis of concentric-tube resonators having unpartitioned cavities, *Journal of the Acoustical Society of America*, 64 (1978), 207–215. <https://doi.org/10.1121/1.381963>
- [22] Abramowitz, M., Stegun, I., *Handbook of Mathematical functions*, Dover, New York, 1964.
- [23] Ayub, M., Tiwana, M.H., & Mann, A.B., Reflection coefficient of a dominant mode in a trifurcated duct of soft walls in the presence of mean flow, *Meccanica*, 48 (2013), 341–349. <https://doi.org/10.1007/s11012-012-9605-7>
- [24] Tiwana, M.H., Nawaz, R., & Mann, A.B., Radiation of sound in a semi-infinite hard duct inserted axially into a larger infinite lined duct, *Analysis and Mathematical Physics*, 7 (2017), 525–548. <https://doi.org/10.1007/s13324-016-0154-4>
- [25] Mitra, R., Lee, S.W., *Analytical techniques in the theory of guided waves*, The Macmillan Company, 1971.